

SURFACE SEGREGATION IN MULTI-COMPONENT SYSTEMS: MODELING
BINARY Ni-Al ALLOYS USING THE BFS METHOD

Azeddine Kasmi, B.S.

Problem in Lieu of Thesis Prepared for the Degree of
MASTER OF SCIENCE

UNIVERSITY OF NORTH TEXAS

August 2004

APPROVED:

Duncan L. Weathers, Major Professor
William Deering, Committee Member
Sam Matteson, Committee Member
Floyd McDaniel, Chair of the Department of
Physics
Sandra L. Terrell, Dean of the Robert B. Toulouse
School of Graduate Studies

Kasmi, Azeddine, Surface Segregation in Multi-component Systems: Modeling Binary Ni-Al Alloys Using the BFS Method. Master of Science (Physics), August 2004, 49 pp., 15 figures, references, 13 titles.

Although the study of surface segregation has a great technological importance, the work done in the field was for a long time largely restricted to experimental studies and the theoretical work was neglected. However, recent improvements in both first principles and semi-empirical methods are opening a new era for surface scientists. A method developed by Bozzolo, Ferrante, and Smith (BFS) is particularly suitable for complex systems and several aspects of the computational modeling of surfaces and segregation, including alloy surface segregation, structure and composition of alloy surfaces and the formation of surface alloys.

In the following work I introduce the BFS method and apply it to model the Ni-Al alloy through a Monte-Carlo simulation. A comparison between my results and those results published by the group mentioned above was my goal. This thesis also includes a detailed explanation of the application of the BFS method to surfaces of multi-component metallic systems, beyond binary alloys.

ACKNOWLEDGEMENTS

I would like to present my greatest respect and thanks to Dr.Duncan Weathers for his guidance and patience. I would like also to thank the members of the committee, Dr. Matteson and Dr. Deering, for their cooperation. Also, special thanks to Dr. Deering for his great job on teaching the core classes.

TABLE OF CONTENTS

	Page
ACKNOWLEDGEMENTS	ii
LIST OF FIGURES	iv
1 INTRODUCTION	1
2 GENERAL CONCEPTS	6
2.1 Introduction.....	6
2.2 Heat of Formation.....	7
2.3 Strain Energy	10
2.4 Chemical Energy.....	16
2.5 Coupling The Strain and Chemical Energy	19
3 APPLICATION OF THE BFS METHOD TO THE CALCULATION OF THE HEAT OF FORMATION OF BCC NI-AL ALLOY	21
3.1 Strain Energy	21
3.2 Chemical Energy.....	24
3.3 Heat of Formation.....	26
3.4 Parametrization of the BFS Method	26
3.5 Results and Discussion	30
4 SURFACE COMPOSITION OF TERNARY ALLOYS	38
4.1 Ni-Al Binary Alloy	43
4.2 Ni-Al+Ti Ternary Alloy.....	45
4.3 Ternary Alloy Ni-Al+Cr	47
4.4 Ternary Alloy Ni-Al+Cu	47
BIBLIOGRAPHY.....	49

LIST OF FIGURES

		Page
1.1	The design is of an empirical nature	3
1.2	The design of an empirical nature is augmented with theoretical modeling	4
2.1	Universal binding relation (E versus r) for a mono-atomic crystal where all the atoms are in their equilibrium lattice sites.....	11
2.2	The reference atom is in the surface	11
2.3	Energy versus radius of an atom in two cases: atom on surface and interstitial atom....	12
2.4	An introduced interstitial atom	13
3.1	Schematic representation of the BFS contributions to the total energy of formation. The left hand side represents the reference atom (denoted by an arrow) in an alloy. The different terms on the right-hand side indicate the strain energy, the chemical energy term and the reference chemical energy	27
3.2	Schematic representation of the contribution of an A atom (center of the cube) to the energy of formation of the B2 A-B compound with lattice parameter a_0 . The left-hand side represents the actual B2 structure. The first term on the right hand side indicates the strain energy environment (all atoms are of type A) in the lattice of the alloy and the second and third terms (between brackets) indicate the chemical energy environment and the reference chemical energy environment, respectively	27
3.3	The energies (strain, chemical, and total) versus the concentration on Ni at T=300 K	32
3.4	The energies (strain, chemical, and total) versus the concentration on Ni at T=1000 K	33
3.5	Energy of the system versus the number of swapping.....	34
3.6	The initial configuration in layers: 16, 17, 18, 19, and 20 as populated randomly	35
3.7	The new configuration after taking into consideration swapping two atoms of different species as mentioned before.....	36
3.8	The energy profile of a film (two surfaces) versus the concentration of Ni.....	37
4.1	Heusler ordering.....	42

CHAPTER 1

Introduction

New high-performance materials have been a goal for a number of industries such as: computer, electronics, military industry, aeronautics, aerospace, etc. for their competitive advantages. For aeronautics and aerospace applications particularly, the potential loss in lives that could occur from any material failure dictates that these systems must be very well understood in order to prevent any disaster. Due to the limitation of defense-related costs after the cold war era, new ways must be developed for industry to assure its growth and at the same time provide significant reductions in expense and cycle time in the development certification processes for new materials. To achieve this goal, the experimental approach to materials research and design must be augmented by computational processes. Developing computational capabilities for alloy design with crystalline materials to the same or greater degree than exists in today's polymer science is the goal of material scientists. In that respect, the BFS method was introduced in early 1990's by:

- 1) Guillermo Bozzolo at Ohio space institute, Cleveland OH.
- 2) John Ferrante at National Aeronautics Space Administration- Lewis Research Center, Cleveland OH.
- 3) John.R.Smith at General Motors Research Laboratories, Michigan.

The design approach is of an empirical nature guided by past experimental work. For most alloy design programs this is essentially one continuous loop (fig 1-a) [5]. An integrated alloy design program that augments experimental results with theoretical modelling would follow the path described in (fig 1-b) [5]. BFS was built by modelling what was known already about the NiAl system. This made it possible for the group to establish more confidence in the model, make changes and optimize the model, and to help understand and interpret the results. Finally, as alloy compositions became more complicated and hard to evaluate, they used the computational model to direct the experimental work and only experimentally verified those few compositions that looked very promising.

The outline of this thesis is as follows : In the first chapter, I introduce the general concepts of BFS method. The notions that are at the heart of alloy formation dynamics are explained. They include the heat of formation, the strain and chemical energies and the coupling of both energies in finding the heat of formation.

The second chapter goes over the same concepts once more but this time the emphasis is on the computational techniques and details on the application to NiAl alloy. I also discuss the results of my computational calculations in this chapter.

The final chapter, Chapter 3 is about the surface formation of ternary alloys and understanding of this phenomena through the BFS method. There are no computational results presented ternary alloys in this thesis but the concept is nevertheless

a)

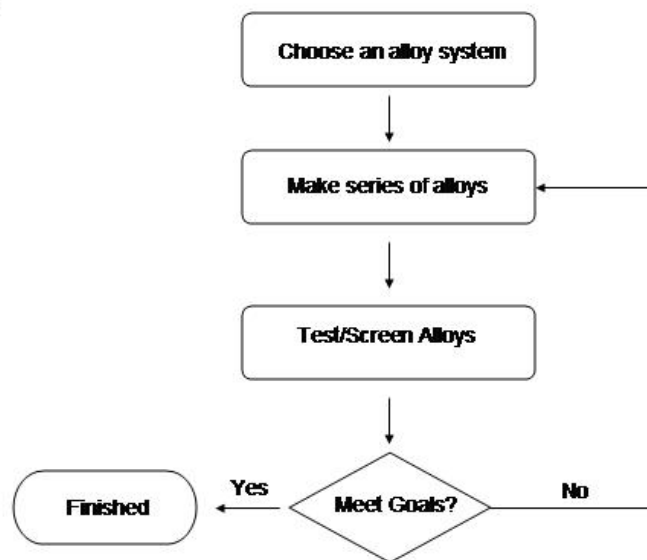


Figure 1.1: The design is of an empirical nature

b)

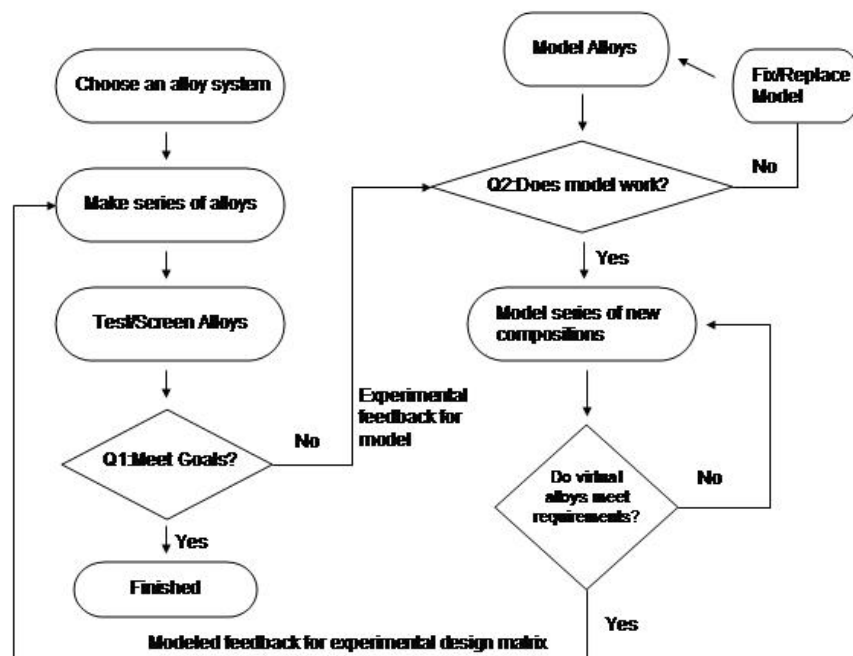


Figure 1.2: The design of an empirical nature is augmented with theoretical modelling

iterated for future research projects.

CHAPTER 2

General Concepts

2.1 Introduction

The BFS method is one of the latest additions to the growing family of quantum-mechanical approximate techniques for the calculation of materials properties. It has a strong foundation in quantum theory, but simplifies the numerical effort usually associated with ab initio methods. While much information about the electronic structure is lost when applying semi-empirical methods to specific systems, valuable understanding of the general behavior of physical systems is gained, since the simplicity of the formulation allows for a quick and sufficiently accurate estimate of general properties. The method is based on the ideas of Equivalent Crystal Theory (ECT) [11] for defect formation energies in elemental solids and uses only pure metal and two alloy properties as input data.

The simplicity of the method relies on the basic assumption that the energy of each non-equivalent atom is described as a superposition of two separate contributions: a strain energy that deals with the structural changes, and a chemical energy that takes into account the changes in chemical composition. The calculation of the strain energy is a straightforward application of equivalent crystal theory for pure elements:

it is computed as if the neighbors of a given atom were of the same atomic species. Therefore, no information for the alloy is needed except for neighbor locations. The calculation of the chemical energy follows an ECT-like format with the introduction of two additional “perturbative” parameters which mimic the interaction between atoms of different atomic species in the overlap region and account for the changes in the electron density due to the presence of the other atomic species. For binary alloys A-B, two such parameters are needed: Δ_{AB} and Δ_{BA} . These two parameters are obtained from two experimental or theoretical alloy properties as input.

2.2 Heat of Formation

The BFS method provides a simple algorithm for the calculation of energy of formation ΔH of an arbitrary alloy. In other words, this is the difference between the energy of the alloy and that of its individual constituents. The BFS method defines the energy of formation as the superposition of individual contributions of all the atoms in the alloy:

$$\Delta H = \sum_i (E'_i - E_i) = \sum_i e_i , \quad (2.1)$$

where

E'_i is the energy of atom i in the alloy, and

E_i is the corresponding value in a pure mono-atomic crystal.

According to first principles, the calculation of ΔH would simply require the computation of the energy of each atom in its equilibrium pure crystal and then its energy in the alloy. Meanwhile, the BFS method avoids a direct computation of the difference e_i for each atom in the alloy. Therefore, a two-step approach for such a calculation was introduced in order to identify contributions to the energy due to structural and compositional effects. As a result of this approach, the individual contributions of each atom e_i to the total energy of formation ΔH of the sample is divided into two components: a strain energy and a chemical energy. A proper coupling of these two apparently independent processes (strain and chemical effects) must be accomplished in order that the final result approaches the result one would obtain if a straightforward calculation (i.e., using ab initio methods) was carried out. The strain energy is defined as the contribution to the energy of formation from an atom in an alloy computed as if all the surrounding atoms were of the same species, while the original structure of the alloy is maintained. Thus, two things can be different between the reference crystal and the alloy. First, atoms of other species may occupy neighboring sites in the crystal. Second, the crystal lattice may not be equivalent in size or structure to that of the ground state crystal of the reference atom. As a conclusion, the strain energy represents only the change in energy due to the change in the geometrical environment of the crystal lattice, ignoring the additional degree of freedom

introduced by the the varying atomic species. Furthermore, the advantages of this assumption are:

1. The fact of transforming the alloy into a mono-atomic crystal gives a great simplification to the calculation of the energy of the reference atom in the alloy structure.
2. It gives partial information concerning only the structure of the alloy, which could serve later to identify fine geometrical effects on structure.

The second contribution to the BFS energy of formation is the chemical energy. In this case, the BFS group isolated the compositional effect of different atoms which occupy sites neighboring the reference atom by leaving out any structural information from the original alloy lattice. This was done by forcing the neighboring atoms to occupy equilibrium lattice sites corresponding to sites in the pure cell of the reference atom but changing the composition of the atoms to match the chemical profile in the alloy lattice. As mentioned earlier, a coupling function shall be introduced. Therefore, the heat of formation of the alloy is written:

$$\Delta H = \sum e = \sum (e_s + ge_c) , \quad (2.2)$$

where

e_s is strain energy,

e_c is chemical energy, and

g is the coupling function and the sum extends over every atom in the alloy.

2.3 Strain Energy

Calculation of the strain energy is a straightforward process and any technique designed to compute the energetics of pure crystals should be appropriate. However, the choice of the appropriate technique should be limited to those that maintain a substantial level of accuracy regardless of the geometry. The first principle calculations would be ideal for this task but the excessive computational effort associated with complex geometries makes this technique not an optimal one. However, in the case of NiAl first principles could be used without any major difficulties due to the simplicity of the NiAl structure. In contrast to the first principle method, ECT [11] provides a simple algorithm for the calculation of defect energies. In terms of the Universal Binding Energy Relation (UBER) [9], consider the ground state crystal, characterized by the equilibrium value of the Wigner-Seitz cell, r_{WSE} .

In the presence of a surface or in the presence of an interstitial atom, a given atom will have a higher energy along the binding energy curve, which also corresponds to a certain ideal perfect crystal with an expanded or compressed lattice parameter.

Any atom in these equivalent crystals has the same energy as those of the reference atoms. The curve indicates that there are two values of the Wigner-Seitz radius for which each atom in a homogeneous ideal crystal has the same energy as the reference

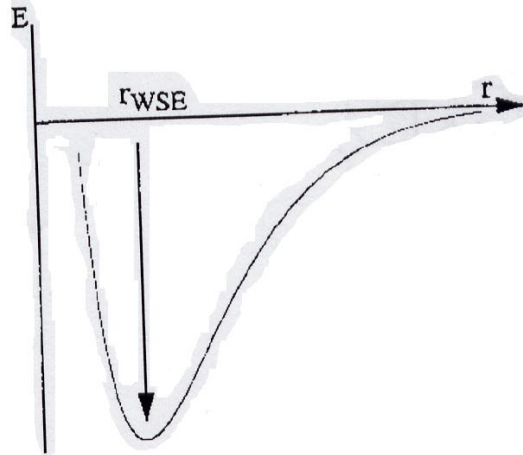


Figure 2.1: Universal binding relation (E versus r) for a mono-atomic crystal where all the atoms are in their equilibrium lattice sites

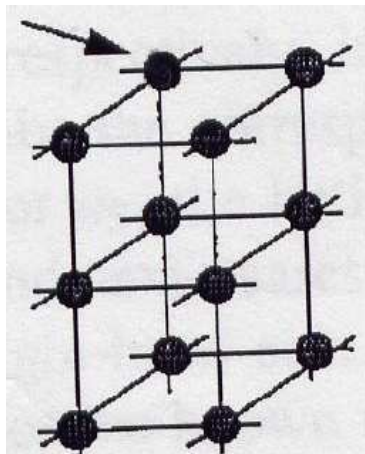


Figure 2.2: the reference atom is in the surface

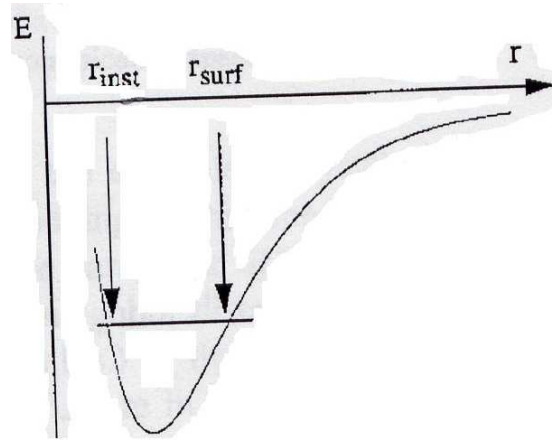


Figure 2.3: Energy versus radius of an atom in two cases: atom on surface and interstitial atom

atom in the defect crystal. These two crystals are called equivalent crystals of the reference atom and the two positions represent two different conditions. To the right of the minimum, the crystal has an increased lattice parameter and thus a reduced electron density. To the left of the minimum the opposite is true. As an example, let us consider an atom on the surface of a metal. The loss of a large number of neighbors will lead to an increase in its energy due to the decrease in electron density. This atom has the same energy in that situation as it would have in a perfect crystal but with a larger lattice parameter. In terms of energy, the atom could not distinguish between being on the surface or being in a larger version of the ground state crystal. Conversely, if an interstitial atom is introduced close to the reference atom, its energy increases to be equivalent to the one it would have in a properly homogeneously compressed ideal crystal. The following figure reiterates these concepts.

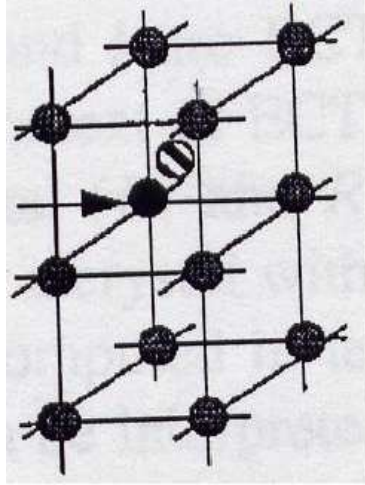


Figure 2.4: An introduced interstitial atom

The surface atom is in an environment of reduced electron density, equivalent to that found in an isotropically expanded bulk crystal. As a consequence, every point along the UBER of a certain crystal is degenerate due to the presence of a large number of defects that would have the same energy and obviously the same equivalent crystal. In other words, the reference atom can be in the presence of a number of different defects that raise its energy by the same amount. Therefore, we can assign the same equivalent crystal to all those defects. ECT provides an efficient algorithm for finding the equivalent crystal for each atom based on quantum perturbation theory [11]. In ECT, it is sufficient in most cases to consider all neighbors up to "second neighbor distance" (nearest neighbors and next-nearest neighbors). Finding the equivalent crystal for a certain atom near a defect is done by finding the

equivalent lattice parameter, i.e, the expanded or compressed lattice parameter of the equivalent crystal in such a way that the energy of an atom in the crystal is the same as that of the atom in the defect crystal. This goal is achieved by solving the following equation for the lattice parameter of the equivalent crystal:

$$NR_1^p \exp(-\alpha R_1) + MR_2^p \exp -(\alpha + 1/\lambda)R_2 = \sum_k r_k^p \exp -(\alpha + S(r_k))r_k , \quad (2.3)$$

where

N is the number of nearest neighbors,

M is the number of next-nearest neighbors in the equivalent crystal,

R_1 is the nearest-neighbor distance in a crystal with lattice parameter a_s , and

R_2 is the next-nearest-neighbor distance in a crystal with lattice parameter a_s .

p , α , λ , and l are ECT parameters that fully describe the corresponding atomic species [11].

The right-hand side (r.h.s) of this equation is computed in terms of the actual distances for the known structure in the defect crystal r_k . Thus, it can be interpreted as a measure of the defect due to the actual atomic environment of the reference atom. r_k are the distances between the atoms of the surrounding and the reference atom. $S(r)$ is a screening function. For the particular case where all the neighboring

atoms are located at lattice sites, $r_j = r_1$ and $S(r_1) = 0$ for nearest neighbors, and $r_j = r_2$ and $S(r_2) = 1/\lambda$ for next-nearest neighbors. The sum runs over all neighboring atoms at distances r_k within a sphere of radius r_c defined as the next nearest-neighbor distance according to ECT. If equation (2.3) has a solution, the strain energy can be written as

$$e_s = -E_c(1 + a_s)\exp(-as)$$

where

$$a_s = q(a_s - a_e)/l,$$

a_e is the equilibrium lattice parameter,

E_c is the cohesive energy of the ground state crystal,

q is the ratio between the equilibrium lattice parameter and the equilibrium Wigner Seitz radius r_{WSE} , and

l is a scaling length.

l can be written as

$$l = \sqrt{(\Delta E/12\pi B r_{WSE})},$$

where

B is the equilibrium bulk modulus, and

ΔE is the cohesive energy.

Thus, we can determine the BFS strain energy contribution of the reference atom as the difference between the energy of the atom in the defect crystal and its energy at equilibrium in its ground state crystal:

$$e_s = E_c(1 - (1 + a_s)\exp(-a_s))$$

2.4 Chemical Energy

To calculate the chemical contribution e_c , as opposed to the strain energy term, the surrounding atoms retain their chemical identity, and they are forced to be in equilibrium lattice sites. The changes in electron density in the overlap between the neighboring atoms are now different from those used in the calculation of the strain energy (where all atoms are of the same atomic species).

These considerations are taken into account by introducing a small perturbation to the parameter α of the reference atom, denoting the fact that a neighboring atom could be a different element. Therefore, new BFS parameters Δ_{AB} (Δ_{BA}) are introduced to denote the influence of a neighbor of species B(A) on the electron density in the vicinity of the reference atom A(B) for the interaction between atoms A and B.

So,

$$\alpha_{AB} = \alpha_A + \Delta_{BA}$$

when the reference atom is of species A and its neighbor of species B.

and

$$\alpha_{BA} = \alpha_B + \Delta_{AB}$$

when the reference atom is of species B and its neighbor of species A.

The BFS parameter Δ_{AB} (Δ_{BA}) perturbs the pure element α , indicating the mixed nature of the bond.

In this sense, the same concepts (the existence of an equivalent crystal) apply except that the reference atom can have different energies than that allowed by its own UBER. As mentioned before, α is the only parameter within this formalism that carries all the information regarding the electron density in the overlap region between a pair of atoms.

In similar fashion to equation (2.3) and taking into account that the neighbor atoms are located in equilibrium lattice sites of a pure crystal of the reference atom, the equation to be solved for the chemical equivalent crystal is:

$$NR_1^p \exp(-\alpha R_1) + MR_2^p \exp-(\alpha + 1/\lambda)R_2 = \sum_k r_{1,A}^{pA} \exp-(\alpha + \Delta_{kA})r_{1,A} + \sum_k r_{2,A}^{pA} \exp-(\alpha + \Delta_{kA} + 1/\lambda_A)r_{2,A} \quad (2.4)$$

where

$r_{1,A}$ is the nearest-neighbor distance in an ideal crystal A,

$R_{2,A}$ is the corresponding next-nearest-neighbor distance,

R_1 is the nearest-neighbor in the equivalent crystal,

R_2 is the next nearest neighbor in the equivalent crystal.

Equation (2.4) is solved for a_c and the scaled lattice parameter a^*_c is given by

$a^*_c = q(a_c - a_A)/l_A$. The chemical energy will be given

$$e_c = \gamma E_c (1 - (1 + a^*_c) \exp(-a^*_c))$$

where

$$\gamma = \begin{cases} 1 & \text{if } a^*_c > 0 \\ -1 & \text{if } a^*_c < 0 \end{cases}$$

Moreover, another term should be introduced into the definition of the chemical energy contribution to account for those situations where the reference atom does not have full coordination, i.e., the number of nearest neighbors is less than that found in the perfect equilibrium crystal. An example would be the reference atoms that occupy a surface site of an alloy. In computing the chemical energy, information about the existence of the surface is introduced by the fact that there are not enough atoms in the vicinity of the reference atom to correspond to the assumptions made for equation (1.4). Therefore, the chemical energy obtained in this way would carry information not only on the chemical effect but also on the structural effect due to the absence of some neighbors. To free the chemical energy from this structural information, the previously defined chemical energy shall be referenced to a similar structural state but

where all the atoms surrounding the reference atom are of the same identity as the reference atom. Thus, the reference chemical energy e_{co} is computed in this manner.

As a consequence, the total chemical energy contribution from the reference atom is

$$\epsilon_c = e_c - e_{co},$$

where

e_{co} is computed by using equation (1.4) but setting the BFS parameters to zero.

2.5 Coupling The Strain and Chemical Energy

As mentioned earlier, the chemical energy does not depend on the actual geometry of the alloy. Therefore, the BFS strain and chemical energy terms need to be coupled properly. In order to describe the asymptotic behavior of such a quantity, i.e., ϵ_c should vanish at large separations and should increase at small separations, a coupling function g linking both terms shall be introduced. This coupling function introduces this asymptotic behavior by the means of scaled lattice parameter $a*_c$. If $a*_s = 0$, then the reference atom finds itself in an environment that resembles equilibrium. If $a*_c > 0$, this results from average expansions with respect to equilibrium and if $a*_c < 0$, this is due to average compressions. Therefore, the coupling function is defined as:

$$g = \exp(-a*_s)$$

It is clear from this expression that the defects that involve expansions reduce the effect of the chemical energy on the total energy of formation:

$$e = e_s + g(e_c - e_{co}) = e_s + g\epsilon_c.$$

CHAPTER 3

Application of the BFS Method to the Calculation of the Heat of Formation of bcc NiAl Alloy

In this chapter, the concepts of the BFS method presented so far will be implemented to calculate the strain energy e_s , chemical energy e_c , and the heat of formation of a binary alloy NiAl in the B2 structure. The β -phase of the binary NiAl system exists over a range of stoichiometry from about 45 to 60 at percentage of Ni [1]. At the stoichiometric composition, NiAl should exist in a perfectly ordered state where the Ni and Al atoms occupy the cube centers of a generalized body-centered cubic lattice.

3.1 Strain Energy

Referring to equation (1.3), one can note that in the actual alloy each Ni atom has 8 nearest-neighbor Al atoms at a distance r_1 and 6 next-nearest-neighbor Ni atoms at a distance a_o . Therefore, the BFS strain energy equation for a Ni atom is:

$$8R_1^{p_{Ni}} \exp(-\alpha_{Ni}R_1) + 6R_2^{p_{Ni}} \exp -(\alpha_{Ni} + 1/\lambda_{Ni})R_2 =$$

$$8r_1^{pNi} \exp(-\alpha_{Ni}r_1) + 6a_o^{pNi} \exp -(\alpha_{Ni} + 1/\lambda_{Ni})a_o. \quad (3.1)$$

The solution of this equation is trivial

$$a_s(Ni) = a_o.$$

So, the BFS strain energy contribution is

$$e_s(Ni) = E_c(Ni)(1 - (1 + a * _s (Ni)) \exp(-a * _s (Ni)))$$

where the scaled lattice parameter of the strain equivalent crystal is given by

$$a * _s (Ni) = q(a_o - a_{Ni})/l_{Ni}.$$

Note that:

a_{Ni} is the lattice constant of the pure Ni crystal

$a_o = 2.871\text{\AA}$ is the lattice constant of the alloy

In the case of an Al atom

$$\begin{aligned} 8R_1^{pAl} \exp(-\alpha_{Al}R_1) + 6R_2^{pAl} \exp -(\alpha_{Al} + 1/\lambda_{Al})R_2 = \\ 8r_1^{pAl} \exp(-\alpha_{Al}r_1) + 6a_o^{pAl} \exp -(\alpha_{Al} + 1/\lambda_{Al})a_o. \end{aligned} \quad (3.2)$$

The solution of this equation is trivial:

$$a_s(Al) = a_o.$$

So, the BFS strain energy contribution is

$$e_s(Al) = E_c(Al)(1 - (1 + a * _s (Al)) \exp(-a * _s (Al))),$$

where the scaled lattice parameter of the strain equivalent crystal is given by:

$$a * _s (Al) = q(a_o - a_{Al})/l_{Al}.$$

The value of q is determined as follows:

In the case of bcc structure the density n_{Ni} of Ni atoms in a pure crystal (n_{Al} in the case of Al pure crystal)is

$$n_{Ni} = 1/((4\pi)/3)r_{WSE}^3 \text{ and } n_{Ni} = 2/a^3,$$

so,

$$2/a^3 = 3/4\pi r_{WSE}^3, \text{ and}$$

$$r_{WSE}^3/a^3 = 3/8\pi.$$

Thus, q is defined as

$$q = r_{WSE}/a = (3/8\pi)^{1/3}.$$

3.2 Chemical Energy

The calculations are particularly simple in the given example since both pure crystals are of the same crystallographic structure as the alloy.

The BFS equation for the calculation of the chemical energy contribution for atom Ni is

$$\begin{aligned} 8R_1^{pNi} \exp(-\alpha_{Ni}R_1) + 6R_2^{pNi} \exp -(\alpha_{Ni} + 1/\lambda_{Ni})R_2 = \\ 8r_{Ni}^{pNi} \exp(-(\alpha_{Ni} + \Delta AlNi)r_{Ni}) + 6a_{Ni}^{pNi} \exp -(\alpha_{Ni} + 1/\lambda_{Ni})a_{Ni}, \end{aligned} \quad (3.3)$$

where

$$R_1 = \sqrt{3}/2a_c, R_2 = a_c, r_{Ni} = \sqrt{3}/2a_{Ni}, \text{ and}$$

r_{Ni} is the equilibrium nearest-neighbor distance in a crystal.

Note that a Ni atom interacts with 8 nearest neighbors of species Al, which explains

the presence of the factor Δ_{AlNi} . The next-nearest neighbors are 6 of the same atomic species Ni.

The equation above is solved (using Newton-Raphson method) [12] [2] for the equivalent lattice parameter a_c and the chemical energy contribution is:

$$e_c(Ni) = \gamma E_c(Ni) (1 - (1 + a *_c (Ni)) \exp(-a *_c (Ni)))$$

where the scaled lattice parameter of the chemical equivalent crystal is given by:

$$a *_c (Ni) = q(a_c - a_{Ni})/l_{Ni}$$

γ is defined as follows

$$\gamma = \begin{cases} 1 & \text{if } a *_c > 0 \\ -1 & \text{if } a *_c < 0 \end{cases}$$

In the case of an Al atom, a similar calculation is performed replacing the appropriate parameters. Note, in particular, that the interaction parameter in the exponential in the first term of the r.h.s of equation (2.3) is now $\alpha_{Al} + \Delta_{NiAl}$, as all the nearest neighbors of the reference Al atom are of species Ni.

3.3 Heat of Formation

In this particularly simple example, there is no need to compute the reference chemical energy e_{co} for either type of atom. This is due to the fact that the corresponding environments correspond to perfect equilibrium Ni and Al crystals already.

Therefore, the total chemical energy contributions are:

$$\epsilon_c(Ni) = e_c(Ni) \text{ and } \epsilon_c(Al) = e_c(Al)$$

Finally, the energy of formation ΔH of the B2 structure Ni-Al will read:

$$\Delta H = (1/2)(e_s(Ni) + g_{Ni}\epsilon_c(Ni) + e_s(Al) + g_{Al}\epsilon_c(Al))$$

The expression above applies only to this stoichiometric binary system characterized by one atom of each atomic species. In more complex situations the calculation might involve considering more non-equivalent atoms. In this example, the Ni atoms locate themselves in one simple cubic sublattice and the Al atoms in the other.

3.4 Parametrization of the BFS Method

The power and accuracy of the BFS method rely not only on the fact of separation between the strain and chemical contributions, but also on the parameters used both for the individual elements (p , l , a_e , E_c , λ) and those used for each type of binary combination that might appear in the system (Δ_{AB} and Δ_{BA}). Also, the Ni-Al example that we have shows clearly the extreme simplicity of the BFS method

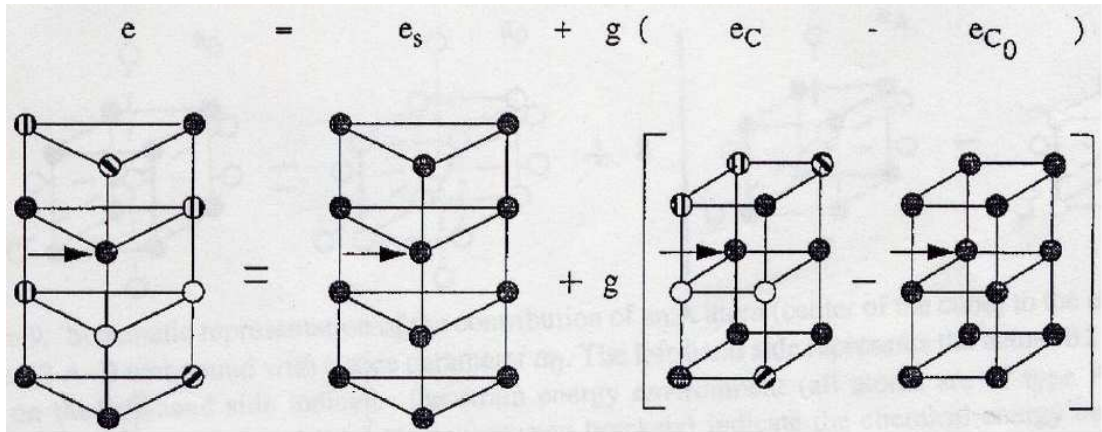


Figure 3.1: Schematic representation of the BFS contributions to the total energy of formation. The left hand side represents the reference atom (denoted by an arrow) in an alloy. The different terms on the right-hand side indicate the strain energy, the chemical energy term and the reference chemical energy.

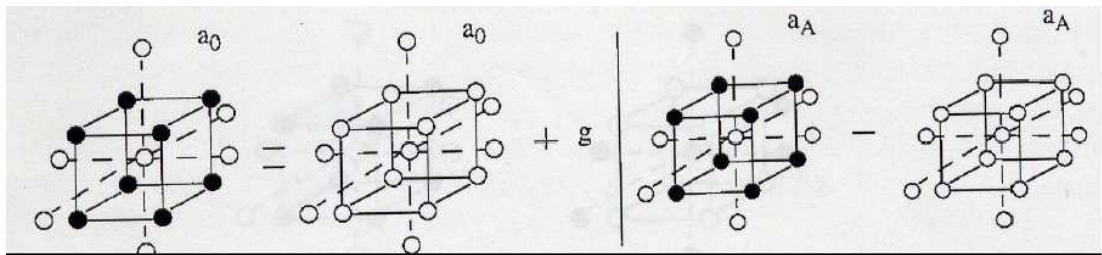


Figure 3.2: Schematic representation of the contribution of an A atom (center of the cube) to the energy of formation of the B2 A-B compound with lattice parameter a_0 . The left-hand side represents the actual B2 structure. The first term on the r.h.s indicates the strain energy environment (all atoms are of type A) in the lattice of the alloy and the second and third terms (between brackets) indicate the chemical energy environment and the reference chemical energy environment, respectively.

when the crystallographic structure of the alloy is the same as that of the constituents (i.e., both Ni and Al are bcc elements and the alloy formed is also bcc-based). As far as the given system of β -Ni-Al is concerned, this binary alloy has a tendency to form in a B2 structure despite the fact that its constituents are fcc elements. Making the assumption that a bcc phase of Ni as well as for Al exists, the complexity of the calculation would be reduced to a level similar to the example just discussed. If the BFS method relied only on experimental input for the determination of the necessary parameters, it would be impossible to implement this approach. However, the determination of the physical properties of these elements (bcc-Ni and bcc-Al) regardless their non existence in nature is carried out by the first principles methods. This approach not only eliminates the dependence of the BFS method on uncertain or non-existent experimental input, it also simplifies the numerical complexity of the problem and introduces a systematic procedure for the generation of the necessary parametrization (i.e., computed by same method, same level of approximation).

The linear-Muffin-Tin-Orbital (LMTO) method in the Atomic Sphere Approximation (ASA) is used to determine these parameters. This method is used to compute: cohesive energy E_c , equilibrium lattice parameter a_e , and bulk modulus B_0 of the elemental solids in the same crystal symmetry as that of the compound(see table 1). The LMTO method uses a minimal basis set. Only the orbitals s,p and d are used and all the calculations were done with equivalent sampling of the Brillouin zone for

the bcc lattice. Table 2 shows the pure element LMTO-generated parameters p , l , E_c , a_e and the resulting value of α for Ni and Al. Also, the BFS formalism allows one to determine the BFS parameters Δ_{AB} and Δ_{BA} by an analytical procedure [5].

atom	lattice const. $a(\text{\AA})$	Cohes. energy $E_c(\text{eV})$	Bulk mod $B_0(\text{GPa})$
Ni	2.752	5.869	249
Al	3.19	3.942	78

Table1.LMTO computed input parameters for Ni-Al calculations

atom	p	α ($1/\text{\AA}$)	l (\AA)	λ (\AA)
Ni	6	3.067	0.763	0.2717
Al	4	1.8756	1.038	0.3695

Table2.ECT computed input parameters for Ni-Al calculations

BFS parameters	
$\Delta_{NiAl} = -0.0581 \text{ \AA}^{-1}$	$\Delta_{AlNi} = 0.0840 \text{ \AA}^{-1}$

Table3.BFS computed input parameters for Ni-Al calculations

3.5 Results and Discussion

The results are obtained by computer simulations based on a Monte Carlo algorithm [8] using the BFS method at each step in the simulation (see the appendix for the code).

Initially a computational cell consisting of 20 layers of 2000 atoms is set up. A starting composition is chosen and each atom within the cell is assigned a species probabilistically. Only the upper 10 layers are “active” .i.e., their compositions are allowed to vary during the computation. As the simulation proceeds, a pair of atoms of opposite species is chosen randomly from within the active region of the computational cell and the total energy of the cell is computed using the BFS method. The chemical species of the two atoms are reversed and the total energy is recomputed. The reversal is accepted if it lowers the energy, or accepted with a probability $\exp(-\Delta E/kT)$ if it raises the energy (ΔE is the difference in energy between the initial and final state) according to the Metropolis criterion. The simulation is continued until the segregation profile attains a steady state (see figure 10).

The following figures show the energies per atom versus the concentration of Ni. According to my results there is a slight segregation of Al atoms on the surface with a higher concentration on the layer just under the surface, please see figures 11 and 12. Also, I simulated the case of a film (two surfaces). In that case I have taken this assumption: the layers 13 to 20 and 1 to 7 are active. In other words, their composition is allowed to change in contrast with the layers 8 to 12 that are considered as a bulk. The results show also a segregation of Al atoms on the surface (see figure 13). Despite the fact that I do not have any results done by the BFS group to compare with mine at this time, I do believe that my results are close to what the BFS group had found or at least I am in the right path.

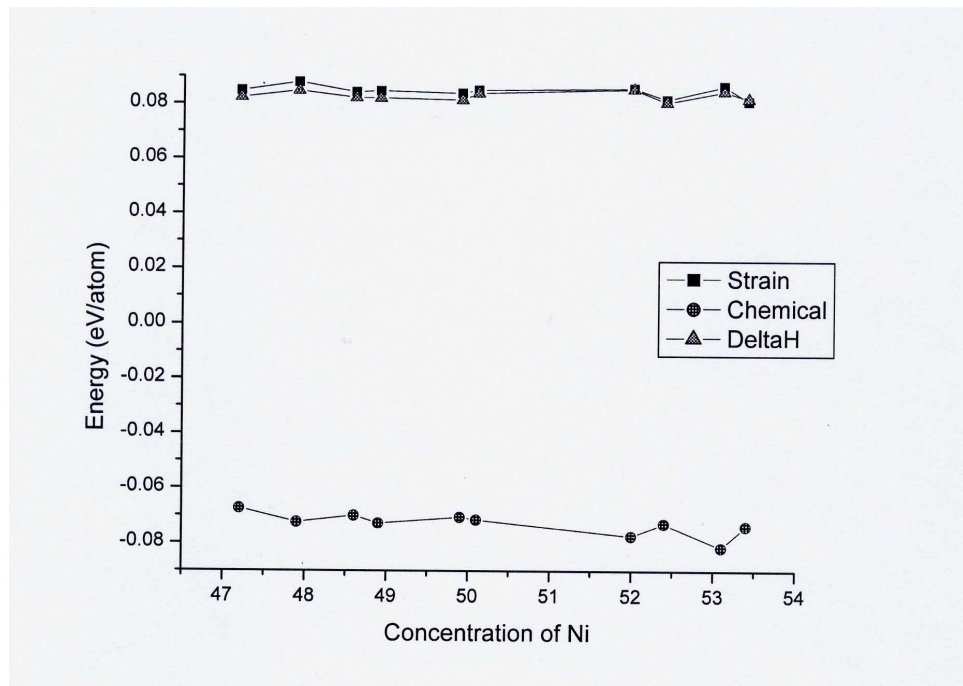


Figure 3.3: The energies (strain, chemical, and total) versus the concentration on Ni at T=300 K.

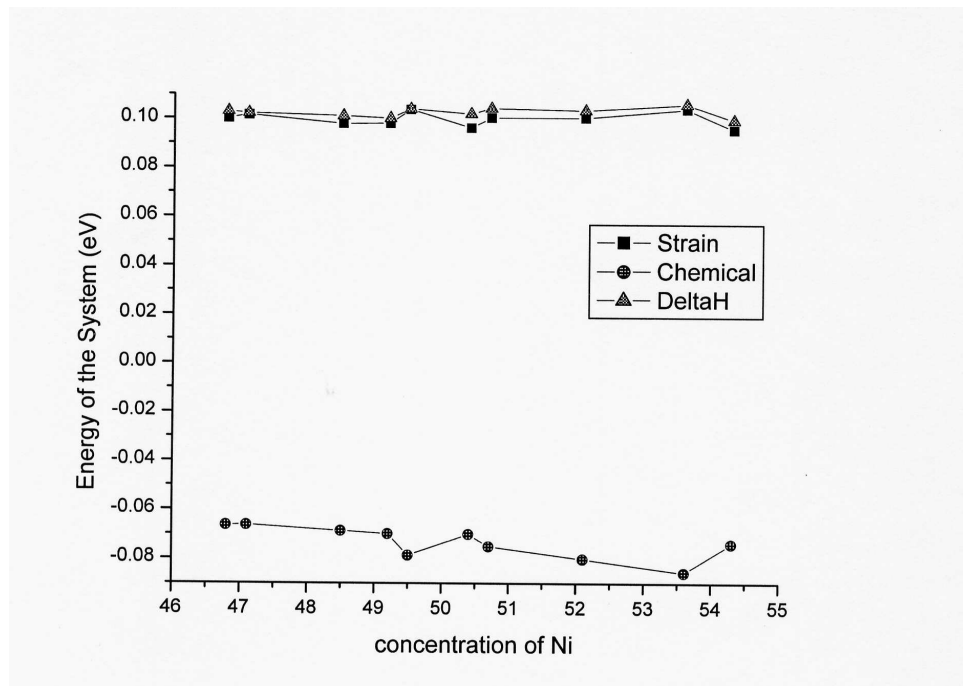


Figure 3.4: The energies (strain, chemical, and total) versus the concentration on Ni at T=1000 K.

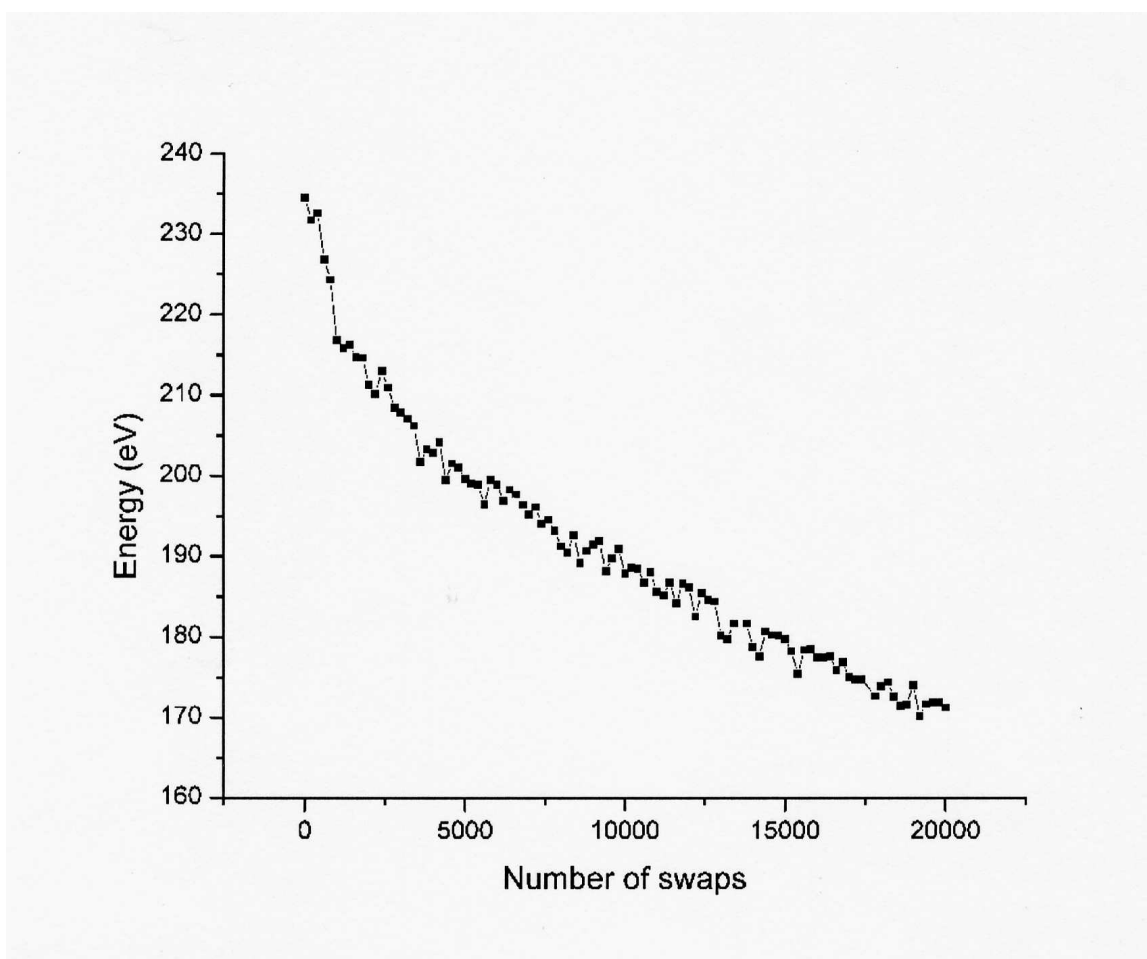


Figure 3.5: Energy of the system versus the number of swapping

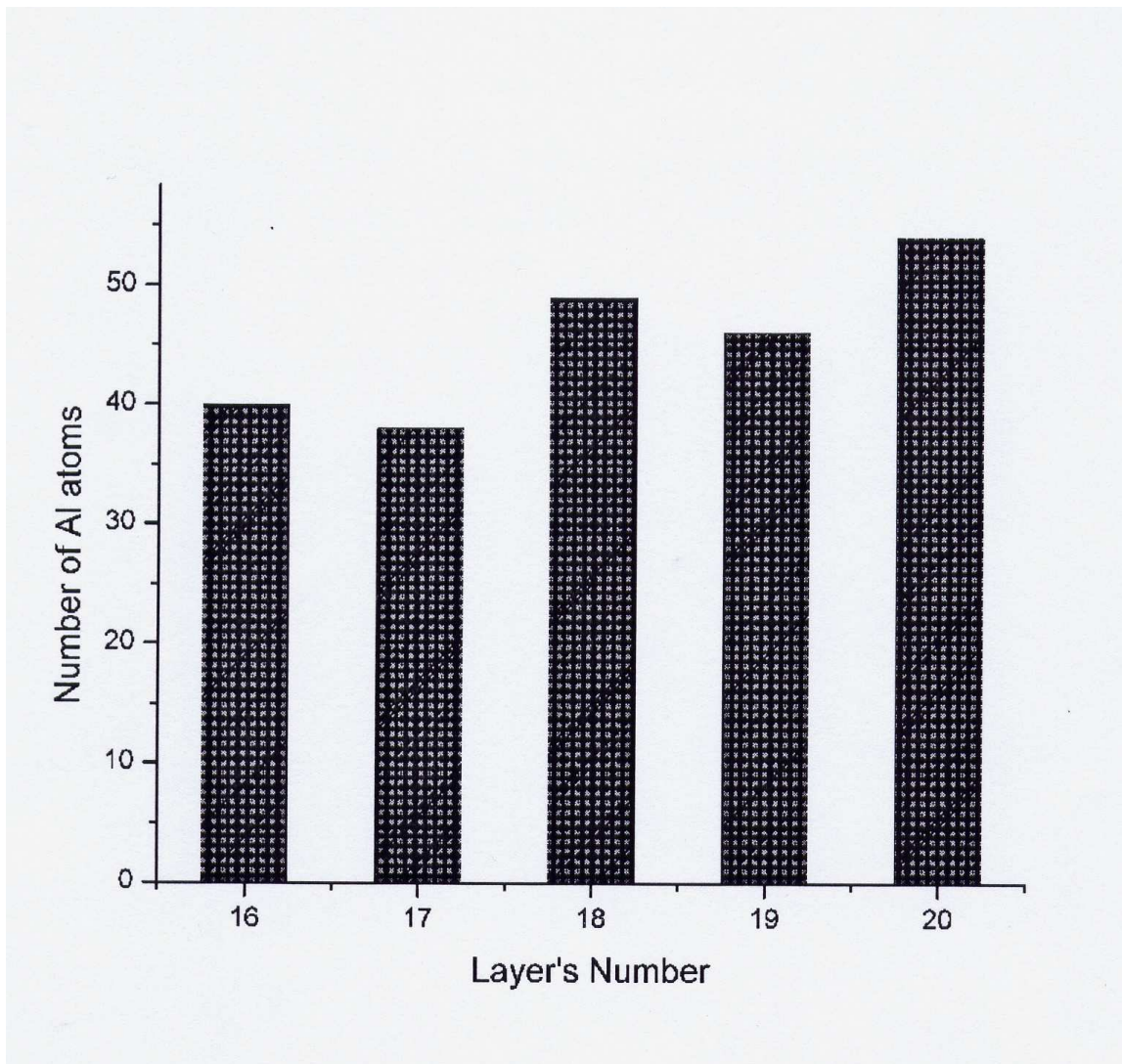


Figure 3.6: The initial configuration in layers: 16, 17, 18, 19, and 20 as populated randomly.

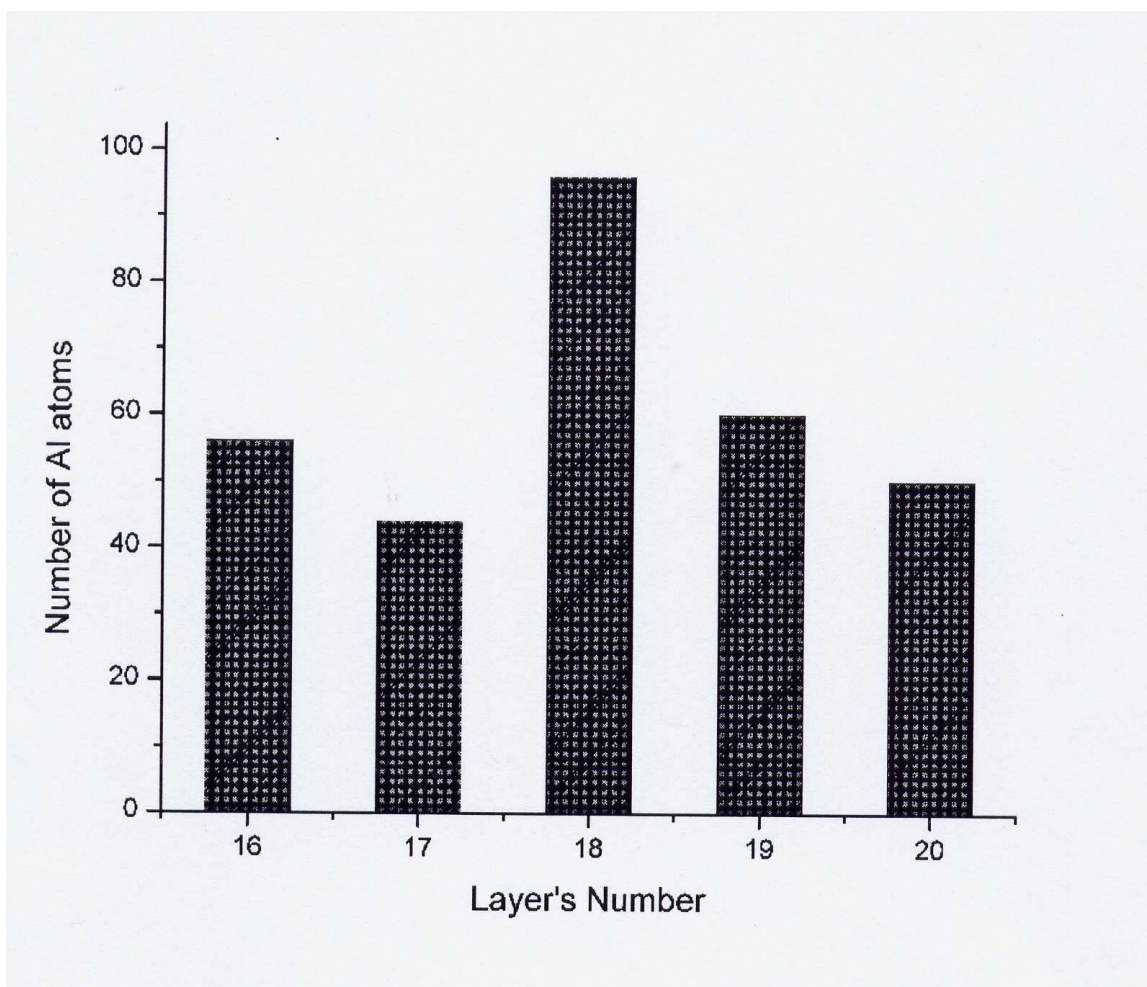


Figure 3.7: The new configuration after taking into consideration swapping two atoms of different species as mentioned before.

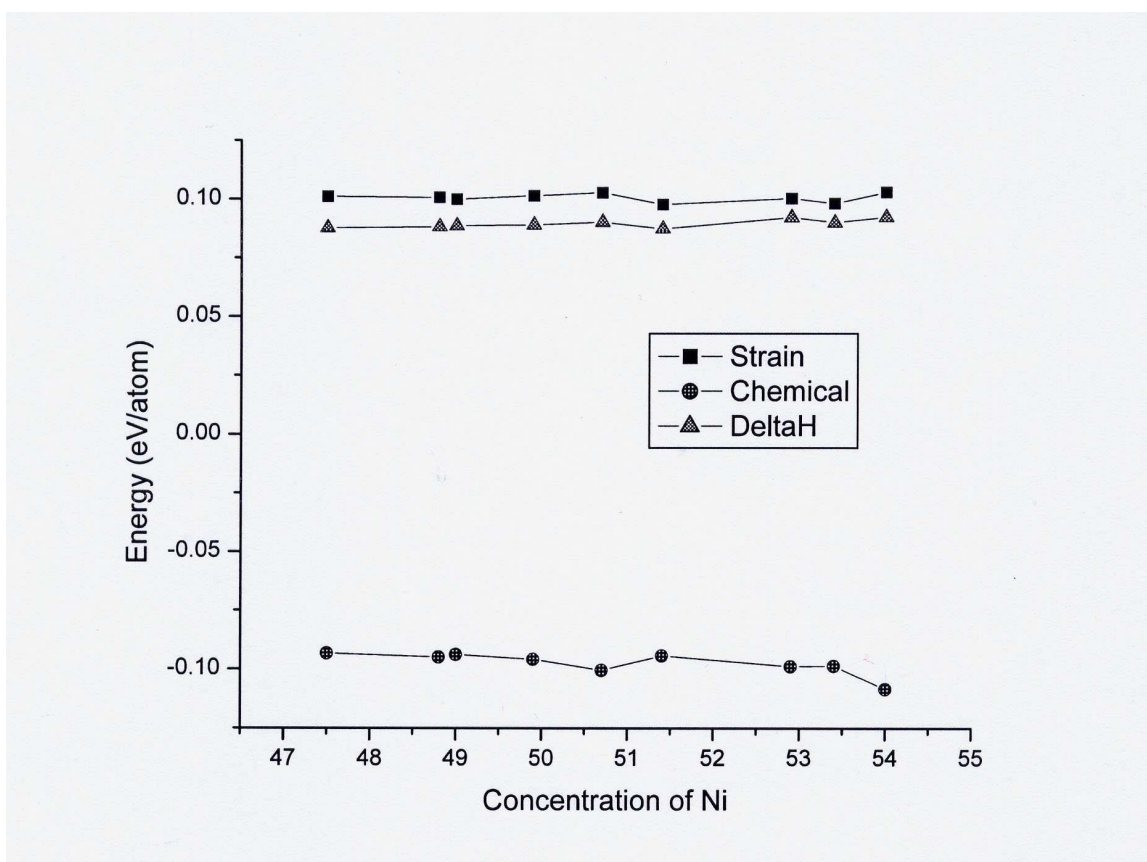


Figure 3.8: The energy profile of a film (two surfaces) versus the concentration of Ni

CHAPTER 4

Surface composition of ternary alloys

The purpose of this section is to show that the BFS method is valid not only for binary alloys but also for multi-component metallic systems (beyond binary alloys). Except for a few comparative theoretical or experimental studies on the binary Ni-Al system, there is almost no other study that deals with these multi-component systems.

The results to be shown consist of the study of the behavior of bcc, fcc and hcp elements in a bcc based alloy. The determination of pure element physical properties for which no experimental values exist have to be determined theoretically. Once again, the Linear-Muffin-Tin-Orbitals (LMTO) method [7] in the atomic sphere approximation is used to compute the necessary parameters. To provide parameters to the BFS method, the calculation of the equilibrium properties of the elemental solid for the same symmetry of the compound to be studied is necessary.

In this case, single element properties (lattice parameter, cohesive energy and bulk modulus) of Ni, Al, Ti, Cr and Cu are calculated in bcc. It's worth mentioning that the BFS approach is parameterized without considering the relaxation caused by the formation of a vacancy, so no relaxation is allowed in the LMTO calculations.

The ECT and BFS parameters used in this work for Ni,Al,Cr,Ti and Cu are listed

in tables 4 and 5. Once these parameters are computed, they remain the same for any calculation involving any of these elements without any further adjustment or replacement.

Atom	Latt.param (\AA)	Ec (eV/atom)	Bo (Gpa)	Vacancy Energy(eV)
Ni	2.752	5.869	249.2	3.0
Al	3.192	3.942	77.3	1.8
Ti	3.213	6.27	121.0	2.0
Cr	2.837	4.981	286.0	4.9
Cu	2.822	4.438	184.5	1.8

Table 4. LMTO results.

p	α ($1/\text{\AA}$)	λ (\AA)	l (\AA)
6	3.0670	0.673	0.2716
4	1.8756	1.038	0.3695
6	2.6805	1.048	0.3728
6	2.8580	0.6460	0.2300
6	3.1082	0.7614	0.2710

Table 5. ECT parameters.

For the determination of Δ_{ij} please see [3].

j_i	Ni	Al	Ti	Cr	Cu
Ni	0.00000	-0.05813	-0.06582	-0.02975	0.02085
Al	0.028220	0.00000	-0.06360	-0.01307	0.05887
Ti	0.45690	0.22830	0.00000	0.06579	0.21964
Cr	0.20480	-0.01637	-0.04691	0.00000	0.02664
Cu	-0.01489	-0.04793	-0.05555	-0.01016	0.00000

Table 6. BFS parameters from LMTO results for bcc-structured alloys.

The entry A_{ij} corresponds to the BFS parameter Δ_{ij} .

The discussion is limited to the results of BFS/Monte Carlo simulations starting with the simple NiAl system, then the ternary Ni-Al-Ti and Ni-Al-Cr systems and finally the quaternary Ni-Al-Ti-Cr. According to [6] in the case of Ni-Al, the results for the (110) surfaces showed no preferential segregation of Al, whereas the (100) surfaces clearly showed Al enrichment. Al segregation would be expected based on surface energy and strain energy considerations. However, Roux and Grabke [10] argue that the Ni-Al binding energy is sufficiently large to overcome these effects. More recent experimental work clearly indicates the segregation of Al to the (001) surface plane of Ni-Al alloys [13]

As mentioned in chapter 2, Ni-Al forms a B2 bcc-based structure, with Ni and Al atoms occupying separate interpenetrating sublattices. Experimental and theoretical

studies coincide in estimating the solubility limit of Ti in Ni-Al to be between 5% and 10% Ti. Beyond the solubility limit, the formation of the ternary-ordered Heusler Ni_2AlTi phase is observed.

The formation of Heusler precipitates has been determined by comparing the energy of formation of every possible arrangement of Ni, Al, and Ti atoms for a wide range of concentrations [6]. It was found that below 5 at % Ti, Ti atoms remain in solid solution in the Ni-Al matrix, whereas above that concentration, the formation of ordered Heusler structures is energetically favored. Moreover, finite temperature Monte Carlo simulations using the BFS method for computing the energy give some indication of the influence of the temperature treatment on the final low temperature state of the alloy where the formation of Heusler precipitates is favored by slow cooling process.

Experimental results performed after the simulations confirm these findings [4]. Three NiAl single crystal alloys (Ni-47Al-3Ti , Ni-45Al-5Ti , and Ni-43Al-7Ti) were grown by a Bridgman technique. The samples were homogenized for 32 hours at 1644 K aged for 6 hours at 1255K and slowly cooled from the aging temperature. The purpose of this heat treatment was to produce a low temperature " equilibrium " microstructure that would best correspond to the ground state condition modeled with the BFS method.

As mentioned before, the geometry to be used in this study by the BFS group is B2

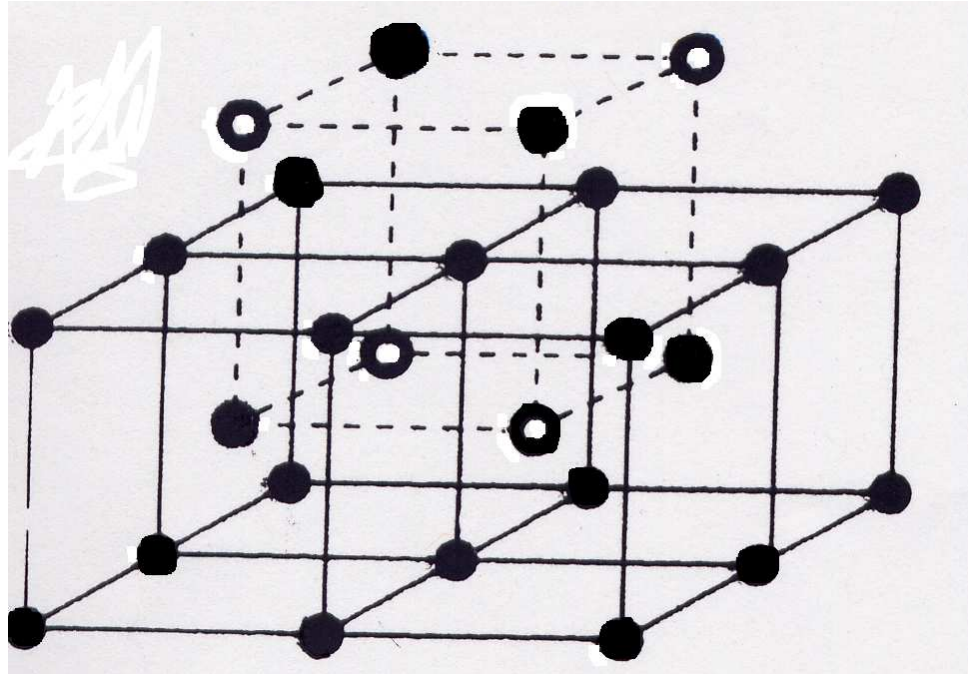


Figure 4.1: Heusler ordering

structure with periodic boundary conditions perpendicular to the (100) faces of the film.

The film thickness ranges from 2.1 nm to 2.2 nm which corresponds to 14 atomic planes. This depends on the number and type of atomic species included. For example:

Film	film thickness (nm)
Ni-33Al-34Cr	2.136
Ni-48Al-2Ti	2.137
Ni-45Al-5Ti	2.146
Ni-40Al-10Ti	2.156
Ni-23Al-10Ti-34	2.147

Table7. This table shows some films studied and their corresponding thickness.

4.1 Ni-Al binary alloy

The most important feature in the film structure is the formation of an Al surface plane on both sides of the film by the motion of Al atoms that were originally in planes close to the surface. Also, very little change in composition is observed in planes near the center of the film which simulate a bulk environment. These results are compatible with experimental results. The way to measure the changes in composition between the bulk and the film cell is given by the coordination matrix. The element of this matrix C_{ij} indicates the probability that an atom of species i has an atom of species j as a nearest neighbor. Thus, a perfect bulk B2 structure would be described by:

$$\begin{pmatrix} 0 & 1 \\ 1 & 0 \end{pmatrix}$$

with the first column and row assigned to Ni and the second to Al. In similar way, the ideal Heusler coordination matrix for Ni_2AlTi is

$$\begin{pmatrix} 0.0 & 0.5 & 0.5 \\ 1.0 & 0.0 & 0.0 \\ 1.0 & 0.0 & 0.0 \end{pmatrix}$$

This means that Al and Ti are located in one sublattice so that they only have Ni atoms as nearest neighbors. Also, Ni atoms are located in the other sublattice with equal number of Al and Ti atoms as nearest neighbors.

For the film cell, the coordination matrix at the final stage of the Monte Carlo simulation is :

$$\begin{pmatrix} 0.27 & 0.73 \\ 0.37 & 0.63 \end{pmatrix}$$

From this matrix we can conclude that mostly pure Al surface planes form by large probability (0.63) of Al-Al nearest-neighbor pairs.

4.2 Ni-Al+Ti ternary alloy

The addition of Ti introduces some changes in the composition of the planes close to the surface. Monte Carlo simulations were conducted for three NiAl-Ti alloys: Ni-47.7Al-2.3Ti , Ni-45Al-5Ti and Ni-40.2Al-9.8Ti [6]. The final state coordination matrices ,with the successive rows and columns correspond to Ni, Al, and Ti respectively, were found to be

$$\begin{pmatrix} 0.2045 & 0.6705 & 0.1250 \\ 0.3114 & 0.6382 & 0.0504 \\ 0.7500 & 0.2500 & 0.0000 \end{pmatrix},$$

$$\begin{pmatrix} 0.2614 & 0.4659 & 0.2727 \\ 0.2344 & 0.6224 & 0.8432 \\ 0.7143 & 0.2857 & 0.0000 \end{pmatrix}, \text{ and}$$

$$\begin{pmatrix} 0.2143 & 0.4643 & 0.3214 \\ 0.2240 & 0.6224 & 0.1535 \\ 0.7167 & 0.2833 & 0.0000 \end{pmatrix}.$$

The first example, Ni-47.7Al-2.3Ti, reproduces the main feature of the previous case (Ni-Al), consisting of the segregation of Al atoms to the surface. Also, the bulk cell contains the Ti atoms in solid solution in the Ni-Al matrix while the thin film displays additional segregation of all Ti atoms to the plane below the surface. Moreover, this effect is more noticeable in the Ni-45Al-5Ti alloy which is the segregation of Ti atoms to the plane below the surface. A few Ti atoms remain in solid solution in the bulk of the film.

Above the solubility limit, the third example Ni-40.2Al-9.8Ti shows the same features described earlier with the addition of the formation of Heusler precipitates in the bulk. The results of two different simulations also suggest that the second plane below the surface remains a pure Ni-Al plane with the formation of Heusler precipitates restricted to the center of the film. This explains the decrease of the element in the coordination matrix C_{NiNi} (0.26) in the case of Ni-45Al-5Ti to 0.21 in the case of Ni-40.2Al-9.8Ti.

For the Ni_2AlTi Heusler alloy, the bulk cell displays the perfect Heusler ordering. In contrast, the film cell once again shows most of the features already seen in the Ni-40.2Al-9.8Ti case: segregation of Al to the surface, segregation of Ti to all Al sites in the second plane and a large number of Heusler precipitates toward the center of the film. Furthermore, there is a noticeable presence of Ti in the top-plane and a Ti depletion in the second plane below the surface.

4.3 ternary alloy Ni-Al+Cr

Cr additions to Ni-Al display a different behavior than that seen in Ni-Al-Ti alloys. The solubility limit of Cr in Ni-Al is between 1 and 2 at % Cr. The alloy Ni-33Al-34Cr is analysed by the BFS group due to the availability of the experimental data for the bulk alloy to compare with. BFS calculations predict a formation of α -Cr precipitates, a feature that is also shown by a slow cooling of the sample. The experimental results also show the formation of dislocation lines due to the misfit between the α -Cr precipitate and the Ni-Al matrix. Therefore, the formation of Cr precipitates should be expected in Ni-rich alloys with Cr additions above the solubility limit. In a film, the Monte Carlo simulation shows three distinctive features:

- (i) Segregation of Al to the surface plane (similar to what we have seen in the previous alloys).
- (ii) The formation of a Cr precipitate immediately below the surface.
- (iii) Some segregation of Cr to the otherwise pure Ni plane in the face of the film opposite to that where the α -Cr precipitate forms.

4.4 ternary alloy Ni-Al+Cu

The last ternary alloy to be discussed is the addition of Cu to Ni-Al. The BFS calculations indicate a weak Cu preference for Al sites with just 0.02 eV energy difference between the Cu(Al) and the Cu(Ni)Al. Simulations were performed for

several films with a computational cell of 960 atoms [6].

The simulations predicts two types of behavior: the state with lowest energy consists of an Al surface plane with all the available Cu atoms occupying sites in this plane. A Ni—Al—Ni stacking pattern follows, where all the Al planes contain some anti-structure Ni atoms. This configuration (the one with the lowest energy) competes with one that is very close in energy but that displays a quite different concentration pattern: the surface plane is pure Al followed by a one-plane mix of all three elements, in turn followed by the bulk Ni—Al—Ni pattern. The likelihood of reaching the high energy state, which is characterized by a pure Al surface plane, decreases with increasing Cu concentration. Effectively, it is observed that above 3 at % Cu all simulations yield the Al+Cu surface plane configuration as the final state. This dual behavior can be explained in terms of strain effect. Both Cu and Al show segregation tendencies in Ni alloy.

BIBLIOGRAPHY

- [1] A Bradley, A.J.and Taylor, Proc.R.soc.A **159** (1939), 232.
- [2] S. C. Chapra and R.P. Canale, *Numerical methods for engineers with programming and software applications*, third ed., McGraw-Hill, Boston, 1998.
- [3] Ronald D. Noebe G. Bozzolo and C.Amador, Computer-Aided Material Design.
- [4] J. Ferrante.A. Garg G.Bozzolo, R.D.Noebe and C. Amador, *was not published at the time*.
- [5] Bozzolo Guillermo, *An introduction to the bfs method and its use to model binary ni-al alloys*, Journal of computer-aided materials design **6** (1999), 1.
- [6] Ronald D.Noebe Brian Good Frank S.Honey and Phillip Abel Guillermo Bozzolo, John Frrante, *Surface segregation in multicomponent systems:modeling of surface alloys and alloy surfaces*, NASA Center for Aerospace Information **209042** (1999), 1–47.
- [7] A.V.Postnikov O.K. Anderson and Savrasov S.Y, Res.Soc.Symp Proc **37** (1992), 253.
- [8] . Rubinstein Reuven Y, *Simulation and the monte carlo method*, John Wiley, New York, 1981.
- [9] Smith J.R.and Ferrante J Rose, J.H., *Universal features of bonding in metals*, Physical Review B **28** (1983), 1835–1845.
- [10] J.P. Roux and H.J.Grabke, Appl. Surf. Sci **68** (1993), 49.
- [11] Perry T. Banerjea A. Ferrante J.and Bozzolo G Smith, J.R., *Equivalent-crystal theory of metal and semiconductor surfaces and defects*, Physical Review B **44** (1991), 6444–6465.
- [12] S. A. Teukolsky W. H. Press, B.P. Flannery and W. T. Vetterling, *Numerical recipes in c The Art of Scientific Computing*, Cambridge University Press, New York, 1989.
- [13] G.N van Wyk E. Taglauer W.D. Ross, J.du Plessis and S. Wolf, Vac. Sci. Technol.A **14** (1996), 1648.